nature materials

ARTICLES

PUBLISHED ONLINE: 28 AUGUST 2011 | DOI: 10.1038/NMAT3101

Spatially controlled simultaneous patterning of multiple growth factors in three-dimensional hydrogels

Ryan G. Wylie[1], Shoeb Ahsan[2], Yukie Aizawa[3], Karen L. Maxwell[4], Cindi M. Morshead[2,5,6] and Molly S. Shoichet[1,2,3,6,7]*

Three-dimensional (3D) protein-patterned scaffolds provide a more biomimetic environment for cell culture than traditional two-dimensional surfaces, but simultaneous 3D protein patterning has proved difficult. We developed a method to spatially control the immobilization of different growth factors in distinct volumes in 3D hydrogels, and to specifically guide differentiation of stem/progenitor cells therein. Stem-cell differentiation factors sonic hedgehog (SHH) and ciliary neurotrophic factor (CNTF) were simultaneously immobilized using orthogonal physical binding pairs, barnase–barstar and streptavidin–biotin, respectively. Barnase and streptavidin were sequentially immobilized using two-photon chemistry for subsequent concurrent complexation with fusion proteins barstar–SHH and biotin–CNTF, resulting in bioactive 3D patterned hydrogels. The technique should be broadly applicable to the patterning of a wide range of proteins.

The ability to localize proteins within 3D scaffolds is critical for spatial control of cellular activities such as cell migration, differentiation and proliferation[1–3]. Neural tissue, such as the retina, is defined by a laminar structure, consisting of multiple cellular layers within a depth of 100–130 μm (ref. 4). Taking advantage of a new multiphoton patterning technique, scaffolds can be created with chemically defined volumes with micrometre resolution, providing a framework for controlled growth and differentiation of stem/progenitor cells (collectively termed precursor cells). Chemically defined volumes of growth factors were selected on the basis of literature precedence to promote differentiation of retinal precursor cells to mature cell types: amino-terminal sonic hedgehog (SHH) for rod photoreceptors[5], and ciliary neurotrophic factor (CNTF) for bipolar cells[6,7] or Müller glia[7,8]. Importantly, several factors, including SHH and CNTF, have been previously shown to remain active when immobilized[9–13]. Furthermore, because SHH is a chemoattractant for adult neural precursor cells (NPCs; ref. 14), we investigated cell migration within 3D photochemically patterned, immobilized-SHH-gradient hydrogels.

To achieve broad applicability, several criteria for protein patterning in hydrogels were required: (1) protein localization must be controlled in three dimensions; (2) multiple proteins must be immobilized simultaneously to avoid protein inactivation over multiple immobilization and washing steps; (3) the system must be applicable to a wide range of proteins. Satisfying these conditions would yield hydrogels with any desired 3D configuration of bioactive proteins as a basis for engineered tissue constructs.

We took advantage of the orthogonal chemistry of peptide binding pairs[15,16] to design hydrogels with 3D immobilized proteins. The binding peptides were first immobilized in defined volumes in the hydrogel using two-photon chemistry[17,18]. Then the candidate factors, expressed as fusion proteins containing the corresponding binding partner, were immobilized. The system is applicable to many proteins by using fusion proteins where one end of the molecule contains the binding domain and the other a biologically active protein, such as a growth factor that guides precursor cell differentiation. The physical binding pairs used herein were barnase–barstar[19,20] and streptavidin–biotin[21] because they form strong complexes with dissociation constants K_d of 10^{-14} M and 10^{-15} M, respectively. Barnase and streptavidin are ideal anchoring proteins because they are stable, which is not true for all proteins, yet it is critical during the fabrication steps of the hydrogel. For example, streptavidin has a high thermal stability with a melting temperature of 75 °C (ref. 22), and barnase readily refolds in the event that it is denatured[23].

An agarose hydrogel was modified with coumarin-caged thiols, which, on two-photon irradiation, are uncaged to yield reactive thiol groups[18]. Agarose was chosen as the hydrogel because it is a transparent scaffold, which is critical to multiphoton chemical patterning[18]. Furthermore, the diffusion of proteins through agarose is sufficient for their introduction and 3D immobilization[24]. 6-bromo-7-hydroxycoumarin was chosen as the thiol-protecting group because it has been previously used with cells and tissue slices[25]. Thiols were selected as the reactive sites because they have been previously shown to be both effective for biomolecule immobilization and non-cytotoxic[3,26]. The thiols act as anchoring sites for the sequential immobilization of both barnase and streptavidin, which were modified to contain thiol

[1]Department of Chemistry, University of Toronto, 80 St George Street, Toronto, Ontario M5S 3H6, Canada, [2]Institute of Medical Sciences, 1 King's College Circle, Room 7213, Toronto, Ontario M5S 1A8, Canada, [3]Department of Chemical Engineering and Applied Chemistry, University of Toronto, 200 College Street, Toronto, Ontario M5S 3E5, Canada, [4]Banting & Best Department of Medical Research, University of Toronto, 112 College Street, Toronto, Ontario M5G 1L6, Canada, [5]Department of Surgery, University of Toronto, 160 College Street, Room 1006, Toronto, Ontario M5S 3E1, Canada, [6]Institute of Biomaterials and Biomedical Engineering, 164 College Street, Room 407, Toronto, Ontario M5S 3G9, Canada, [7]The Donnelly Centre, 160 College Street, Room 514, Toronto, Ontario M5S 3E1, Canada. *e-mail: molly.shoichet@utoronto.ca.

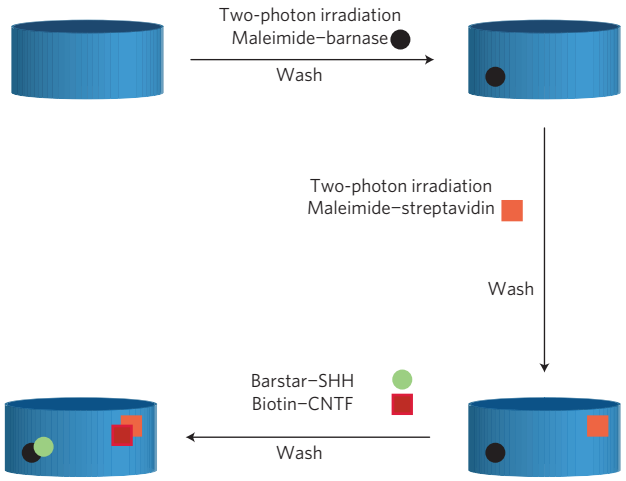

Figure 1 | Method for the simultaneous immobilization of SHH and CNTF. Maleimide-barnase (black circle) is immobilized using two-photon photochemistry and a femtosecond laser. The hydrogel is then washed in buffer to remove unbound maleimide-barnase. Next maleimide-streptavidin (orange square) is immobilized using two-photon irradiation followed by another washing step. The fusion proteins barstar-SHH (green circle) and biotin-CNTF (red square) are soaked into the gel and bind to barnase and streptavidin, respectively. After washing out excess protein, both SHH and CNTF are simultaneously and independently immobilized in three dimensions.

reactive maleimides. Two-photon patterning affords 3D control because of the limited excitation volume. As shown schematically in Fig. 1, maleimide–barnase is photochemically immobilized in the hydrogel, which is washed to remove unreacted maleimide–barnase, and then maleimide–streptavidin is immobilized using the same photochemistry, but in spatially distinct volumes. After washing out the unreacted maleimide–streptavidin, the fusion proteins barstar–SHH and biotin–CNTF are soaked into the gel simultaneously, and specifically bind to immobilized barnase and streptavidin, respectively. A final washing step is carried out to remove unbound proteins, yielding two immobilized bioactive factors in spatially defined volumes within the agarose hydrogel (see Methods). This methodology was tested for each factor individually, facilitating quantification and bioactivity of the immobilized protein, and then for both factors together, demonstrating the power of this technique for simultaneous protein immobilization.

To spatially control the immobilization of SHH to agarose, barstar–SHH and barnase–agarose were synthesized and then the two reacted. The fusion protein barstar–SHH was expressed in *Escherichia coli* and then labelled with the fluorescent Alexa 488 before reaction with agarose–barnase. To synthesize the latter, barnase was expressed in *E. coli*[20,27], followed by modification with sulphosuccinimidyl-4-(N-maleimidomethyl)cyclohexane-1-carboxylate, yielding maleimide–barnase that reacted readily with deprotected agarose–coumarin sulphides (Fig. 2a; see Supplementary Information for further details).

The synthesis of barnase–agarose was a multistep process, involving first synthesis of coumarin-protected agarose sulphide[18], then selective deprotection (in defined volumes) of the coumarin groups by pulsed Ti–sapphire laser and finally reaction of these reactive agarose sulphides with maleimide–barnase. A 1 wt% (wt/vol.) coumarin sulphide agarose hydrogel was synthesized with 2.8% of the agarose repeat units modified with coumarin sulphide and then mixed with maleimide–barnase, before casting as a gel. By controlling the exposure of defined agarose volumes to the Ti–sapphire pulsed laser at 740 nm, the number of photo-exposed agarose-sulphide groups and thus the amount of maleimide–barnase immobilized was varied. Moreover, by simply varying the number of laser scans over a selected volume, the concentration of SHH–barstar immobilized to streptavidin–barnase was controlled.

As shown in Fig. 2, barstar–SHH was immobilized in spatially defined volumes of agarose–barnase. A series of squares, patterned 400 μm below the surface of the hydrogel, demonstrates that the amount of irradiation correlates with the amount of protein immobilized. Ten boxes of 100 μm by 100 μm by ~40 μm (depth) were patterned in the presence of maleimide–barnase with an increasing number of laser scans, from 10 to 46 per box, washed to remove unreacted maleimide–barnase and cleaved coumarin molecules, and then immersed in a solution of barstar–SHH–488 for 16 h. The gel was thoroughly washed to remove excess barstar–SHH–488 and visualized using confocal microscopy (Fig. 2b). The fluorescence intensity was converted to amount immobilized by comparison with a calibration curve (see Supplementary Information for more detail) and plotted as a function of the number of scans in a given volume (Fig. 2c). Interestingly, after 10 laser scans 12 nM of SHH were immobilized, and after 46 scans 134 nM of SHH were immobilized. A linear relationship between number of scans and amount of immobilized SHH was observed. 12 nM represented the lowest concentration that could be imaged, not the lowest concentration that can be immobilized, because the quantification was restricted by the detection limit of the confocal microscope. The concentration of immobilized SHH can be further controlled by varying both the substitution rate of coumarin sulphide on agarose and the laser intensity. The distribution of immobilized barstar–SHH in the z plane within the agarose gel was demonstrated by plotting the fluorescence profile of barstar–SHH–488 against distance along the z axis. The point of irradiation (maximum fluorescence) was arbitrarily set to 0 micrometres for graphical representation. The fluorescent intensity profile of the z axis for all boxes spans approximately 40 μm (Fig. 2d), which represents the best resolution that can be achieved in the z axis. The profile of fluorescence along the z axis broadened with scan number because the excitation volume of the two-photon laser increased with amount of irradiation; however, a 5 μm resolution can be achieved in the x–y plane when patterning fluorescent molecules[18]. These data demonstrate that the coumarin sulphide photochemistry combined with the barnase–barstar system enables 3D immobilization of proteins.

The stability of agarose-immobilized SHH was investigated by measuring the SHH concentration before and after immersion in phosphate-buffered saline (PBS). After 14 d in PBS, there was no statistically significant change in concentration of SHH–agarose (Supplementary Fig. S1), indicating that the barnase–barstar interaction is a suitable physical interaction for stable protein immobilization. This complements the streptavidin–biotin complex, which has been previously shown to be effective for stable biomolecule immobilization in hydrogels[18,28].

To spatially control the immobilization of CNTF to agarose, biotin–CNTF and streptavidin–agarose were synthesized and then the two reacted (Fig. 3a), following a similar overall strategy as described with barstar–SHH and barnase–agarose. Mouse CNTF with the biotinylation sequence, GLNDIFEAQKIEWHE (ref. 29), and a histidine tag at the carboxy terminus was expressed in *E. coli* from a pET-24d vector[30] and purified before biotinylation with the *E. coli* biotinylation enzyme. The protein was then covalently modified with the fluorescent Alexa 633 tag to enable visualization once immobilized to agarose–streptavidin (see Supplementary Information for further details).

To visualize 3D-immobilized fluorescently tagged CNTF, a series of boxes was patterned in the agarose gel, with number of scans varying from 1 to 19 (Fig. 3b). As was observed in the barstar–barnase system, increasing the number of scans with the

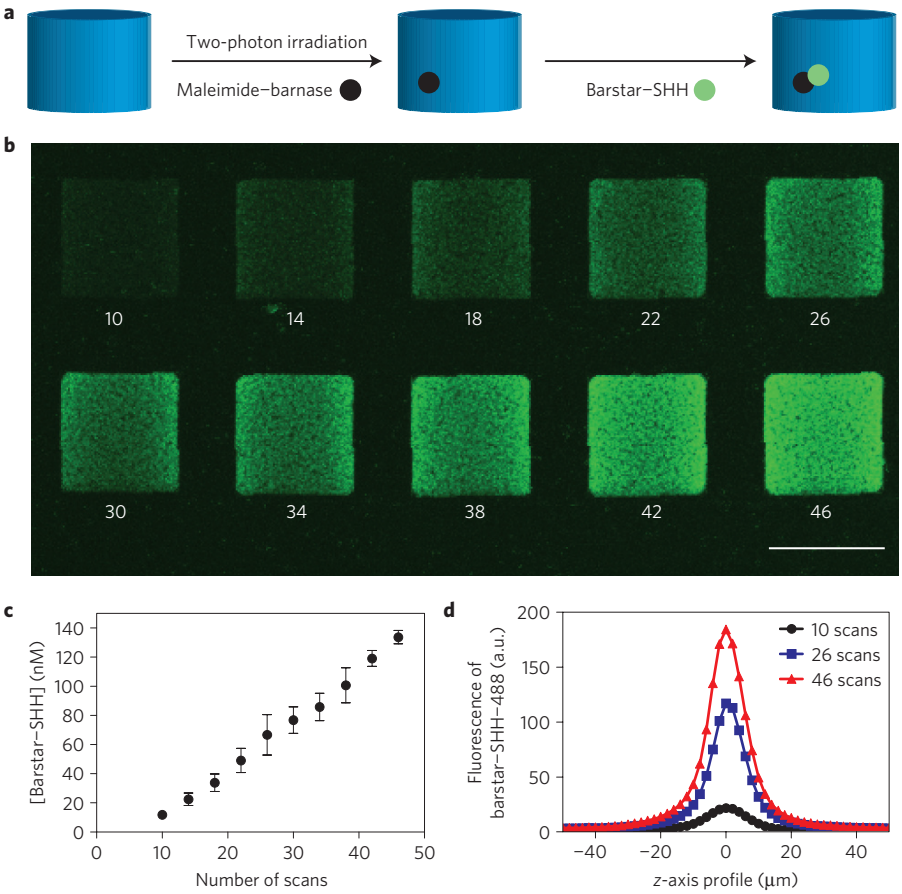

Figure 2 | 3D immobilization of barstar–SHH–488 using barnase–barstar. a, Maleimide–barnase (black circle) was immobilized in a coumarin sulphide agarose gel, followed by the addition of barstar–SHH (green circle) modified with Alexa 488. **b**, Ten different squares 100 × 100 μm with heights of 20–40 μm were patterned 400 μm below the surface of the gel, with each square being scanned a different number from 10 to 46 scans. Scale bar, 100 μm. **c**, The amount of barstar–SHH–488 immobilized versus number of scans was quantified by measuring the fluorescence from each box and compared against a standard curve of coumarin sulphide agarose gels with known concentrations of Alexa 488 (mean ± s.d., $n = 3$). **d**, The *z*-axis profile of fluorescence of barstar–SHH–488 for boxes with 10, 26 and 46 scans, with the maximum intensity centred at 0 μm.

multiphoton Ti–sapphire pulsed laser (at 740 nm) led to increased immobilized CNTF, on the basis of increased agarose sulphides available to bind maleimide–streptavidin and then biotin–CNTF. The concentration of immobilized CNTF was determined by fluorescence to vary between 20 nM and 80 nM as a function of scan number (Fig. 3c). The fluorescence profile along the *z* axis for biotin–CNTF was quantified using the same method as described for barstar–SHH. The fluorescence intensity profile of the *z* axis for the box increased with number of scans from approximately 40 μm for 1 scan to 100 μm for 19 scans, with the peak fluorescence centred at 0 μm (Fig. 3d). The resolution in the *z* axis decreased (broadened) in the streptavidin–biotin system compared with that of barnase–barstar. Because the same photochemistry was used for both methods, the difference in resolution is probably a consequence of the binding interactions having different valences.

Interestingly, similar amounts of barnase (11.9 ± 2.3 nM) and streptavidin (15.8 ± 4.8 nM) were immobilized with comparable laser scan numbers of 10 and 9, respectively, yet significantly different concentrations of SHH and CNTF were immobilized owing to the different binding capacities of barnase–barstar and streptavidin–biotin. For example, the ten scans required to immobilize barnase resulted in 11.9 ± 2.3 nM of barstar–SHH whereas the nine scans used to immobilize streptavidin resulted in 63.0 ± 4.8 nM of biotin–CNTF. Streptavidin has four binding sites for biotin[31,32] whereas barnase has only one binding site for barstar, thus accounting, in part, for the different concentrations of immobilized factors. In this way, we were able to vary the multivalency of grafted proteins between our systems, which has previously been shown to be important for protein potency on linear polymer chains[33].

The simultaneous 3D immobilization of proteins was achieved with SHH and CNTF by taking advantage of orthogonal chemistry with the selective protein binding pairs, barnase–barstar and streptavidin–biotin (Fig. 1). By first immobilizing maleimide–barnase to distinct volumes of coumarin-deprotected agarose sulphide, washing extensively, and then repeating with maleimide–streptavidin, the agarose hydrogel was synthesized for 3D patterning with the barstar and biotin binding partners. A coumarin sulphide agarose hydrogel with maleimide–barnase in PBS at pH 6.8 was patterned with a truncated circular shape, figuratively representing the globe of an eye. A series of four identical shapes was patterned into the agarose hydrogel by scanning 40 times across this shape with the Ti–sapphire laser: each layer was separated by 100 μm in depth, with the deepest layer being 700 μm below the surface of the gel. The gel was washed thoroughly in PBS at pH 6.8 to remove any unreacted maleimide–barnase and then re-patterned in the presence of maleimide–streptavidin. To immobilize maleimide–barnase in the appropriate volume, attaining the desired final shape, the loss of coumarin fluorescence due to maleimide–barnase immobilization was first imaged with the confocal microscope. The laser was then focused in the proper volume to immobilize

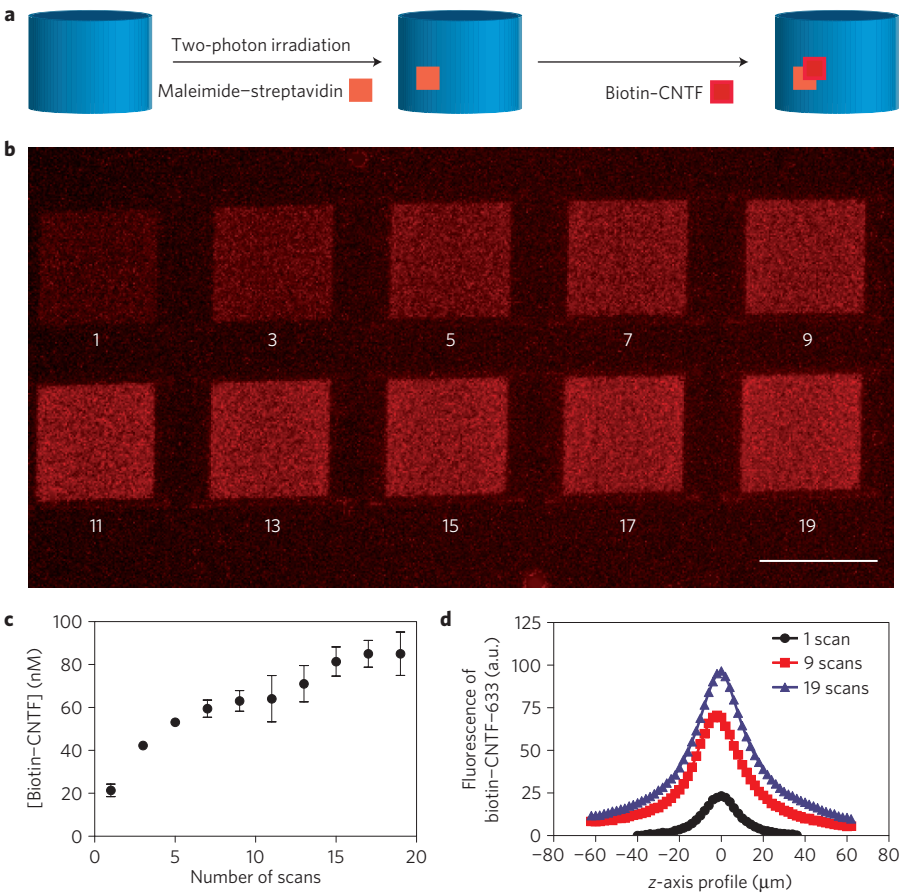

Figure 3 | 3D immobilization of biotin–CNTF–633 using biotin–streptavidin. a, Maleimide–streptavidin (orange square) was immobilized in a coumarin sulphide agarose gel, followed by the addition of biotin–CNTF (red square) modified with Alexa 633. **b**, Ten different regions of boxes of 100 μm × 100 μm with heights of 40–80 μm were patterned 400 μm below the surface of the gel, with each region being scanned a different amount from 1 to 19 scans. Scale bar, 100 μm. **c**, The amount of biotin–CNTF–633 immobilized versus number of scans was quantified by measuring the fluorescence from each box and compared with a standard curve of coumarin sulphide agarose gels with known concentrations of Alexa 633 (mean ± s.d., $n = 3$). **d**, The *z*-axis profile of fluorescence of biotin–CNTF–633 for boxes with 1, 9 and 19 scans, with the maximum intensity centred at 0 μm.

maleimide–streptavidin (Fig. 4a). The maleimide–streptavidin was patterned in an oval shape, within the pocket of the truncated circle of maleimide–barnase, figuratively representing the lens of the eye. The maleimide–streptavidin was immobilized in four distinct volumes with 15 scans per layer of the Ti–sapphire multiphoton laser. More scans were used to immobilize maleimide–barnase than maleimide–streptavidin, on the basis of the results with single-protein patterned volumes.

The 3D patterned agarose hydrogel, with distinct volumes of barnase and streptavidin, was simultaneously modified with barstar–SHH–488 and biotin–CNTF–633 by simply immersing the hydrogel in a solution containing both proteins. Importantly, barstar–SHH and biotin–CNTF were selectively immobilized in distinct volumes, following the agarose-immobilized patterns of barnase and streptavidin, respectively.

Figure 4b shows a confocal micrograph of the first layer of the pattern, with barstar–SHH (green) and biotin–CNTF–633 (red). This image overlaps with that of the loss of coumarin fluorescence from the patterning steps with the laser, demonstrating spatial control through multiphoton irradiation. The 3D reconstructed view, showing each of the four patterned volume layers, demonstrates our ability to pattern both proteins simultaneously in three dimensions (Fig. 4c,d). The fluorescence intensity for each layer of SHH–488 seems to decrease with depth even though the same number of scans was used: the fluorescence at a depth of 400 μm in the gel is more intense than that at 700 μm because the laser intensity during both excitation and emission is attenuated as a function of depth owing to increased scattering of light. The decrease in fluorescence was not observed for CNTF–633 (Supplementary Fig. S2), indicating that the two-photon patterning remains consistent over the depths investigated. The attenuated fluorescence observed for SHH–488 was not observed for CNTF–633 probably because longer wavelengths scatter less light than shorter wavelengths. This suggests that the majority of fluorescence loss for SHH–488 as a function of depth is not from the photochemistry used for immobilization, but rather an artefact of the imaging process (Supplementary Fig. S2).

The beauty of this technique is its simplicity. It can be applied to a broad range of proteins for multiple simultaneous patterning and, importantly, can be achieved with the multiphoton laser of a confocal microscope. Any protein that can be expressed as a fusion protein, with the appropriate binding partner, can be immobilized. Therefore this system can be applied to numerous applications involving 3D cell culture. We have demonstrated the strength of this technique with two proteins, but recognize that more proteins can be immobilized simultaneously with the immobilization of other binding partners. Furthermore, we have demonstrated that concentration gradients of proteins can be patterned (Figs 2 and 3), which is useful for cell guidance. Because all but the final washing step is complete before protein immobilization, the risk of denaturing or degrading the proteins during immobilization is significantly diminished. If the proteins were immobilized sequentially, then those proteins immobilized

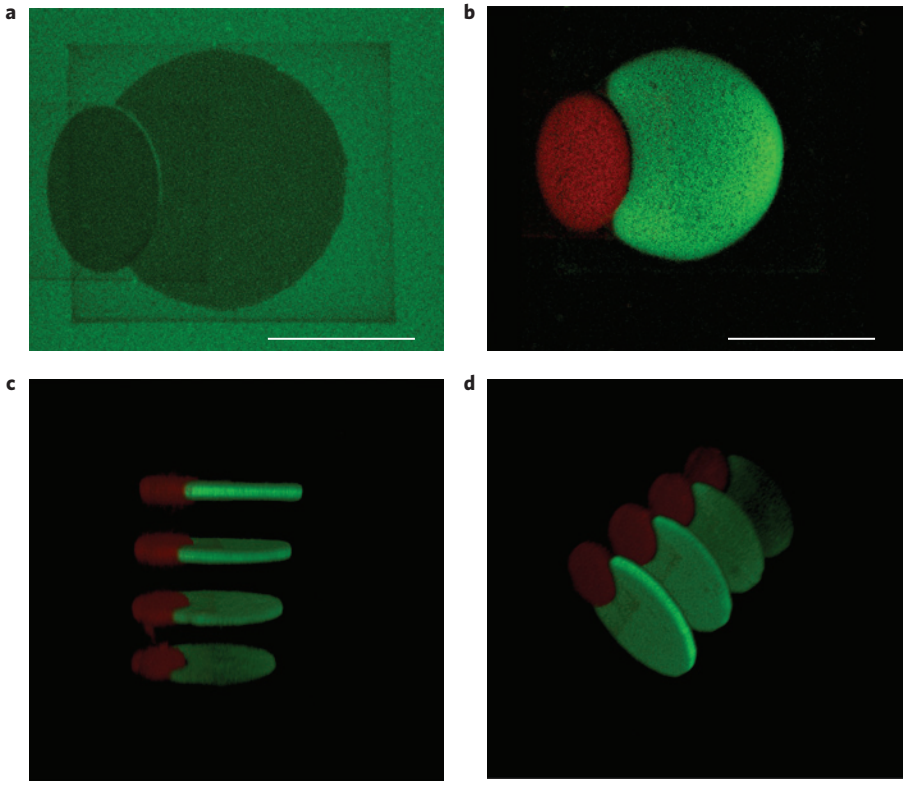

Figure 4 | Representative figures for the simultaneous 3D patterning of biotin–CNTF–633 and barstar–SHH–488. Maleimide–barnase was patterned in layers in the shape of a truncated (green) circle 400, 500, 600 and 700 μm below the surface of the hydrogel with 40 scans per layer. Maleimide–streptavidin was then patterned in a smaller (red) oval shape inserted into the truncated circle of the maleimide–barnase pattern. The oval was patterned with 15 scans in four layers, following the identical method for maleimide–streptavidin. Barstar–SHH–488 and biotin–CNTF–633 were immobilized by simply immersing the hydrogel in solutions of the proteins. **a**, A confocal micrograph showing the loss of coumarin fluorescence of the layer at 400 μm from patterning of maleimide–barnase and maleimide–streptavidin. Scale bar, 100 μm. **b**, A confocal micrograph of the layer at 400 μm demonstrating the localization of barstar–SHH–488 and biotin–CNTF–633 to the volumes patterned. Scale bar, 100 μm. **c**, 3D projection of the reconstructed stack using Image J 3D viewer rotated to see the layers. **d**, The same projection as in **c** viewed from a different angle. Biotin–CNTF–633 in red; barstar–SHH–488 in green.

first might be completely or partially inactive by the time the final protein is immobilized. With the proteins added at the final step, we are more confident in their bioactivity. Thus simultaneous protein immobilization obviates numerous sequential immobilization and washing steps, which had been the state of the art before this study. Moreover, because the immobilization is governed by specific physical interactions, many potential side-reactions are eliminated. For example, by reacting agarose thiols with maleimide-binding partners, side-reactions such as disulphide bonds between proteins and agarose thiols are obviated.

Having demonstrated the patterning chemistry, we tested the bioactivity of the immobilized proteins. Because we are interested in the nervous system, we tested bioactivity with retinal precursor cells (RPCs) derived from the ciliary margin of the adult mouse retina[34]. We examined the activation of SHH and CNTF signalling pathways in cells exposed to the immobilized proteins by plating RPCs on the surface of functionalized hydrogels. All agarose hydrogel scaffolds were chemically modified with the cell-adhesion peptide GRGDS (ref. 35), because agarose itself is non-adhesive and the bioactivity and cell-survival assays to test for possible cytotoxic effects could not be carried out on a non-cell-adhesive substrate[3,9].

RPCs were first shown to express an SHH receptor, Ptch1, by PCR with reverse transcription (RT-PCR) (Fig. 5a), which on SHH binding leads to the upregulation of the transcription factor Gli2 (ref. 36). To test the bioactivity of the immobilized SHH fusion protein, RPCs were screened for the expression of Gli2 by RT-PCR. Gli2 expression was evident for both agarose–barnase–barstar–SHH (with GRGDS) and agarose–GRGDS plus soluble wild-type SHH, but not for agarose–barnase (with GRGDS only; Fig. 5b). These data demonstrate that the immobilized SHH fusion protein, expressed in *E. coli*, is bioactive. Assays for potential cytotoxicity compared cell survival on agarose–barnase–barstar–SHH (with GRGDS) to agarose–barnase (with GRGDS) and agarose–GRGDS. The PicoGreen assay[37] was used to determine the relative amount of double-stranded DNA (dsDNA) as a measure of viable cells after 7 d in culture. The number of viable cells in all groups was not significantly different ($p > 0.05$), demonstrating no toxic effect of the immobilization method used for SHH in the cultures (Fig. 5c). A live/dead stain (calcein AM/ethidium homodier-1) of the RPCs demonstrated that the percentage of live cells varied between 70 and 80% with no statistical significance between groups, further demonstrating the coupling method is non-toxic (Supplementary Fig. S3). It is important to realize that we anticipated a decrease in cell number relative to the number plated, even after 7 d of culture, because many of the cells are lost during plating[38].

To test the bioactivity of agarose-immobilized CNTF, RPCs were first shown to express the CNTF receptor (CNTFR) by RT-PCR (Fig. 5d). To monitor CNTFR activation, we followed the expression of phosphorylated STAT3, a well-known downstream effector of CNTF–CNTFR binding[7,8,39]. Importantly, RPCs stained positive with anti-phospho-STAT3 for immobilized and soluble CNTF and not for controls that lacked CNTF (Fig. 5e). These results demonstrate that our CNTF fusion protein expressed in *E. coli* remained bioactive after immobilization and was able to

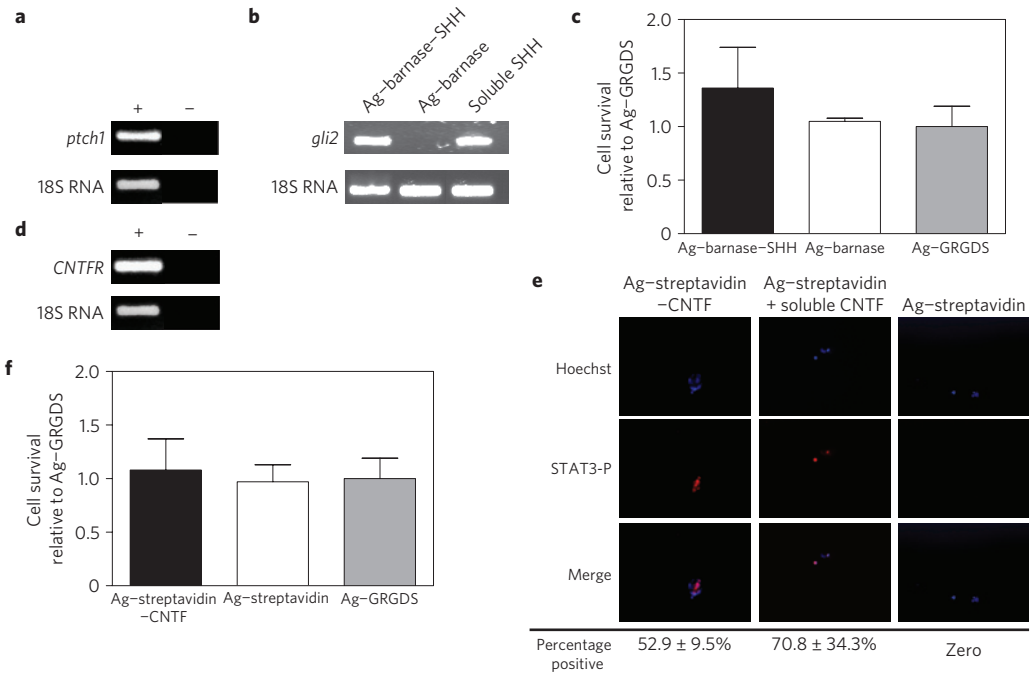

Figure 5 | SHH and CNTF signalling pathways are activated in RPCs that are cultured on immobilized SHH and CNTF, respectively. a, RPCs were assayed for the presence of the *Ptch1* receptor in the SHH pathway using RT-PCR. **b**, RPCs upregulate a key SHH signalling mediator, *Gli2*, in response to immobilized SHH as assayed by RT-PCR. Ag, agarose. **c**, No cytotoxic effect was found by comparing the survival of RPCs cultured on agarose–barnase–SHH (with GRGDS), agarose–barnase (with GRGDS) and agarose–GRGDS. Cell numbers were measured after 7 d by total dsDNA content using the PicoGreen assay (mean ± s.d., $n = 5$ with 5,000 cells per gel). No significant difference was observed between groups using one-way analysis of variance with Tukey's post hoc analysis ($p > 0.05$). **d**, RPCs were assayed for the presence of CNTF receptor, *Cntfr*, by RT-PCR. **e**, RPCs respond biologically to immobilized CNTF. This was determined through immunostaining for phosphorylated STAT3, a protein activated through phosphorylation on CNTF ligand binding to CNTFR. RPCs cultured on gels with either immobilized CNTF or soluble CNTF both stained positive for STAT3-P, whereas gels with only streptavidin and GRGDS did not stain for STAT3-P. The percentage of immunostained cells was calculated, as written below each series of images, and shown to be not statistically different ($p > 0.05$, $n = 5$ samples, mean ± s.d.). **f**, The survival of RPCs cultured on agarose–streptavidin–CNTF (with GRGDS), agarose–streptavidin (GRGDS) and agarose–GRGDS was similar. Cell numbers were quantified after 7 d by the amount of dsDNA present using the PicoGreen assay (mean ± s.d., $n = 5$ with 5,000 cells per gel). No significant difference was observed between any groups using one-way analysis of variance with Tukey's post hoc analysis ($p > 0.05$).

activate the CNTF signalling pathway. Cell viability assays to test for potential cytotoxicity were carried out using the PicoGreen and live/dead assays, and demonstrated that RPCs cultured for 7 d on agarose–streptavidin–biotin–CNTF (with GRGDS) versus agarose–streptavidin (with GRGDS) versus agarose–GRGDS had similar cell viabilities ($p > 0.05$, Fig. 5f; Supplementary Fig. S3). Moreover, the RPC viability on the CNTF gels was not significantly different from that on the SHH gels ($p > 0.05$). These results confirm that barstar–SHH and biotin–CNTF remain bioactive after immobilization, capable of downstream signalling similar to that observed with soluble controls. Our data are consistent with previous results demonstrating that SHH and CNTF remain bioactive after immobilization, albeit with different chemistry and other cell types[12,13].

To gain greater insight into cell migration into the patterned agarose hydrogel, an immobilized gradient of barstar–SHH in GRGDS–agarose was photochemically patterned using an identical synthetic procedure. Using Alexa 488 SHH, the protein gradient was quantified over the first 100 μm, relative to a calibration curve, to be 100–500 ng ml^{-1} (Fig. 6a). NPCs from the subventricular zone, which are known to migrate along an SHH gradient[14], were plated on SHH-gradient GRGDS–agarose gels and compared with GRGDS–agarose. Interestingly, we observed cellular migration predominantly into patterns that contained SHH gradients (to a depth of 85 μm, Fig. 6b), which is a depth appropriate for thin tissues, such as the retina. Only limited migration was observed into channels with only GRGDS (to a depth of 20 μm, Fig. 6c). To facilitate visualization of the migrating cells, NPCs expressing yellow fluorescent protein were shown to migrate into SHH-gradient GRGDS–agarose gels (Fig. 6d). These data demonstrate that 3D penetration of cells into photochemically patterned agarose gels is facilitated with chemoattractant molecules, such as SHH. These data are consistent with previous results, where a concentration gradient of an immobilized vascular endothelial growth factor was required to guide endothelial cells into an agarose hydrogel[26].

Defining the cellular microenvironment is becoming increasingly important as we design *in vitro* systems to better predict *in vivo* response and engineer *de novo* tissues. Designing the 3D scaffold with the appropriate chemical and physical properties is the first step to understanding the cues important to cell survival and stimulation. For example, these 3D biomimetic hydrogels can be used to begin to emulate the complexity of the stem-cell niche, presenting extracellular matrix mimetics, growth factors and mechanical stimuli similar to native tissue while also enabling co-culture of multiple cell types. As the 3D imaging tools continue to advance, probing cells in three dimensions will be facilitated and will open high-throughput (or high-content) screening protocols to advanced 3D patterned hydrogels. Moreover, 3D protein patterning has applications in regenerative medicine, where tissues are engineered *in vitro* before transplantation. Here the agarose hydrogel serves as a blank canvas in which proteins are patterned, demonstrating our ability to create chemically complex scaffolds that will be used ultimately to spatially guide cell fate.

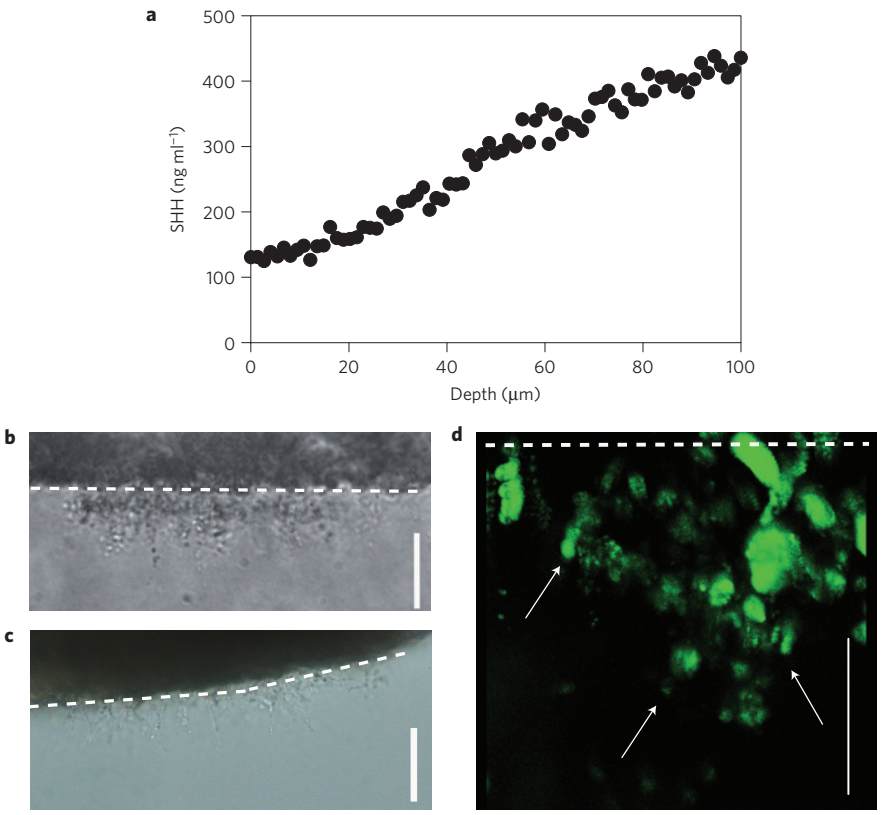

Figure 6 | NPCs migrate into a channel of SHH with RGD. a, Quantification of the concentration profile of SHH-488 as a function of depth within the hydrogel from the surface of the gel to a depth of 100 μm. **b**, Bright-field image of SHH-RGD channel showing that NPCs have migrated into the agarose gel after 14 d to a depth of 85 μm. **c**, Bright-field image of RGD-only channel showing that only minimal migration was observed within the hydrogel after 14 d to a depth of 20 μm. Mostly processes were observed within the gel. **d**, Confocal micrograph of SHH-RGD channel emphasizing migration of NPCs expressing yellow fluorescent protein into the agarose gel. All scale bars represent 50 μm. For all cell images the white dashed line represents the surface of the gel.

Methods

Photopatterning and imaging. All patterns were created and imaged on a Leica TCS-SP2 confocal microscope equipped with an argon laser (50 mW; 458, 476, 488, 514 nm), a red HeNe laser (10 mW; 633 nm), a multiphoton Mai Tai laser using a ×20 objective (NA = 0.4) and an electronic stage. For patterning experiments, the multiphoton laser was set to 740 nm with an offset of 75% and gain of 0% for visualization and an offset of 75% and gain of 43% for patterning. One scan of a 100 μm × 100 μm square takes 1.28 s. A typical patterned hydrogel of ten squares (Figs 2 and 3) took between 2 and 6 min. The maximum length scale that can be achieved (maximum depth of patterning) is limited by the working distance of the lens (15 mm). Leica software version 2.5.1227a was used for the visualization and fluorescence quantification. Z-stacks and 3D images were constructed using Image J.

Patterning SHH–barstar. 25 μl of 1 wt% coumarin sulphide agarose gels with 0.15 mg ml^{-1} of maleimide–barnase was patterned and reacted for 2 h at room temperature (RT) in a humidity chamber. The series of boxes was created by selecting a 100 μm by 100 μm squares, with a height of ~20–40 μm, 400 μm below the surface of the hydrogel. Using a macro, the first box was scanned ten times followed by a further four scans for each subsequent box. The gels were then washed in 200 ml of PBS for 1 d. 20 μl of 0.3 mg ml^{-1} SHH–barstar–488 was placed on top of the gel and left overnight at RT. The gels were washed in PBS at pH 7.4 for 2 d, changing the PBS daily. For the quantification, a z-stack was imaged spanning 182 μm with 2 μm steps and six scans per slice. The 458, 476, 488 nm excitation wavelengths were set to 100% and the gain of the photomultiplier tube was 602 with wavelengths from 500 to 590 nm collected.

Patterning biotin–CNTF. 25 μl of 1 wt% coumarin sulphide agarose gels with 1 mg ml^{-1} of maleimide–streptavidin was patterned and reacted for 2 h at RT in a humidity chamber. A series of boxes was created by selecting a 100 μm by 100 μm square, with a height of ~40–80 μm, 400 μm below the surface of the hydrogel. Using a macro, the first box was scanned once followed by a further two scans for each subsequent box. The gels were then washed in 200 ml of PBS at pH 7.4 for 1 d. 20 μl of 0.54 mg ml^{-1} biotin–CNTF–633 was placed on top of the gel and left for 16 h at RT. The gels were washed again in PBS at pH 7.4 for 2 d, changing the PBS once. For the quantification, a z-stack was imaged spanning 163. 2 μm with 2 μm steps and six scans per slice. The 633 nm excitation wavelength was set to 100% and the gain for the photomultiplier tube at 591 with wavelengths from 640 to 750 nm collected.

Dual patterning. A 25 μl gel of 1 wt% coumarin sulphide agarose with 0.15 mg ml^{-1} of maleimide–barnase was patterned. The truncated circle was selected, after which the region was scanned 40 times. This was repeated three more times with each 100 μm below the previous pattern to construct the layered pattern. After 2 h in a humidity chamber, the gel was washed in PBS at pH 6.8 for 2 h. A solution of 20 μl of 2 mg ml^{-1} of maleimidopropionic acid in PBS at pH 6.8 was added on top of the gel. After 16 h the gel was washed for 1 d in PBS at pH 6.8. 20 μl of 2 mg ml^{-1} maleimide–streptavidin in PBS at pH 6.8 was added on top of the gel at 4 °C. After 16 h, the gel was patterned again by selecting an oval region fitting into the truncated circle and scanned 15 times. This was repeated for each layer of the barnase pattern. The gel was then washed in 200 ml of PBS at pH 7.4 for 1 d. A 20 μl solution of 0.3 mg ml^{-1} of both barstar–SHH–488 and biotin–CNTF–633 was added on top of the gel. After 1 d, the gel was washed for 2 d in PBS at pH 7.4, changing the buffer once. A 327.6 μm stack was constructed with 2.1 μm spacing between slices using the following settings: lasers 458, 476, 488 and 633 nm set to 100%; six scans per slice; collected wavelengths of 500–590 nm and 640–800 nm; photomultiplier tubes of 683 and 589 for green and red channels, respectively.

Migration of NPCs into SHH–RGD channel. NPCs were placed on top of hydrogels with patterns consisting of an SHH gradient with GRGDS or GRGDS alone. After 14 d, hydrogels were imaged and cell migration into the hydrogel was compared between conditions (greater detail is provided in Supplementary Information).

Received 17 September 2010; accepted 18 July 2011; published online 28 August 2011

References

1. DeForest, C. A., Polizzotti, B. D. & Anseth, K. S. Sequential click reactions for synthesizing and patterning three-dimensional cell microenvironments. *Nature Mater.* **8,** 659–664 (2009).

2. Lee, S. H., Moon, J. J. & West, J. L. Three-dimensional micropatterning of bioactive hydrogels via two-photon laser scanning photolithography for guided 3D cell migration. *Biomaterials* **29,** 2962–2968 (2008).
3. Luo, Y. & Shoichet, M. S. A photolabile hydrogel for guided three-dimensional cell growth and migration. *Nature Mater.* **3,** 249–253 (2004).
4. Pires, I., Bernardes, R. C., Lobo, C. L., Soares, M. A. & Cunha-Vaz, J. G. Retinal thickness in eyes with mild nonproliferative retinopathy in patients with type 2 diabetes mellitus: Comparison of measurements obtained by retinal thickness analysis and optical coherence tomography. *Arch. Ophthalmol.* **120,** 1301–1306 (2002).
5. Levine, E. M., Roelink, H., Turner, J. & Reh, T. A. Sonic hedgehog promotes rod photoreceptor differentiation in mammalian retinal cells *in vitro*. *J. Neurosci.* **17,** 6277–6288 (1997).
6. Zahir, T., Klassen, H. & Young, M. J. Effects of ciliary neurotrophic factor on differentiation of late retinal progenitor cells. *Stem Cells* **23,** 424–432 (2005).
7. Bhattacharya, S., Das, A. V., Mallya, K. B. & Ahmad, I. Ciliary neurotrophic factor-mediated signaling regulates neuronal versus glial differentiation of retinal stem cells/progenitors by concentration-dependent recruitment of mitogen-activated protein kinase and Janus kinase-signal transducer and activator of transcription pathways in conjunction with Notch signaling. *Stem Cells* **26,** 2611–2624 (2008).
8. Goureau, O., Rhee, K. D. & Yang, X. J. Ciliary neurotrophic factor promotes Muller glia differentiation from the postnatal retinal progenitor pool. *Dev. Neurosci.* **26,** 359–370 (2004).
9. Aizawa, Y., Leipzig, N., Zahir, T. & Shoichet, M. The effect of immobilized platelet derived growth factor AA on neural stem/progenitor cell differentiation on cell-adhesive hydrogels. *Biomaterials* **29,** 4676–4683 (2008).
10. Leipzig, N. D., Xu, C., Zahir, T. & Shoichet, M. S. Functional immobilization of interferon-gamma induces neuronal differentiation of neural stem cells. *J. Biomed. Mater. Res. A* **93,** 625–633 (2010).
11. Rahman, N., Purpura, K. A., Wylie, R. G., Zandstra, P. W. & Shoichet, M. S. The use of vascular endothelial growth factor functionalized agarose to guide pluripotent stem cell aggregates toward blood progenitor cells. *Biomaterials* **31,** 8262–8270 (2010).
12. Ho, J. E., Chung, E. H., Wall, S., Schaffer, D. V. & Healy, K. E. Immobilized sonic hedgehog N-terminal signaling domain enhances differentiation of bone marrow-derived mesenchymal stem cells. *J. Biomed. Mater. Res. A* **83,** 1200–1208 (2007).
13. Nakajima, M. *et al.* Combinatorial protein display for the cell-based screening of biomaterials that direct neural stem cell differentiation. *Biomaterials* **28,** 1048–1060 (2007).
14. Angot, E. *et al.* Chemoattractive activity of sonic hedgehog in the adult subventricular zone modulates the number of neural precursors reaching the olfactory bulb. *Stem Cells* **26,** 2311–2320 (2008).
15. Zhang, K. C., Diehl, M. R. & Tirrell, D. A. Artificial polypeptide scaffold for protein immobilization. *J. Am. Chem. Soc.* **127,** 10136–10137 (2005).
16. Zhang, K. C., Sugawara, A. & Tirrell, D. A. Generation of surface-bound multicomponent protein gradients. *ChemBioChem* **10,** 2617–2619 (2009).
17. Wylie, R. G. & Shoichet, M. S. Two-photon micropatterning of amines within an agarose hydrogel. *J. Mater. Chem.* **18,** 2716–2721 (2008).
18. Wosnick, J. H. & Shoichet, M. S. Three-dimensional chemical patterning of transparent hydrogels. *Chem. Mater.* **20,** 55–60 (2008).
19. Deyev, S. M., Waibel, R., Lebedenko, E. N., Schubiger, A. P. & Plückthun, A. Design of multivalent complexes using the barnase · barstar module. *Nature Biotechnol.* **21,** 1486–1492 (2003).
20. Hartley, R. W. Barnase–barstar interaction. *Methods Enzymol.* **341,** 599–611 (2001).
21. Weber, P. C., Ohlendorf, D. H., Wendoloski, J. J. & Salemme, F. R. Structural origins of high-affinity biotin binding to streptavidin. *Science* **243,** 85–88 (1989).
22. González, M. *et al.* Interaction of biotin with streptavidin. *J. Biol. Chem.* **272,** 11288–11294 (1997).
23. Khan, F., Chuang, J. I., Gianni, S. & Fersht, A. R. The kinetic pathway of folding of barnase. *J. Mol. Biol.* **333,** 169–186 (2003).
24. Liang, S. *et al.* Protein diffusion in agarose hydrogel *in situ* measured by improved refractive index method. *J. Control. Release* **115,** 189–196 (2006).
25. Furuta, T. *et al.* Brominated 7-hydroxycoumarin-4-ylmethyls: Photolabile protecting groups with biologically useful cross-sections for two photon photolysis. *Proc. Natl Acad. Sci. USA* **96,** 1193–1200 (1999).
26. Aizawa, Y., Wylie, R. & Shoichet, M. Endothelial cell guidance in 3D patterned scaffolds. *Adv. Mater.* **22,** 4831–4835 (2010).
27. Hartley, R. W. *et al.* Barstar inhibits extracellular ribonucleases of streptomyces and allows their production from recombinant genes. *Protein Peptide Lett.* **3,** 225–231 (1996).
28. Lagunas, A., Comelles, E. M. & Samitier, J. Universal chemical gradient platforms using poly(methyl methacrylate) based on the biotin–streptavidin interaction for biological applications. *Langmuir* **26,** 14154–14161 (2010).
29. Cull, M. G. & Schatz, P. J. Biotinylation of proteins *in vivo* and *in vitro* using small peptide tags. *Methods Enzymol.* **326,** 430–440 (2000).
30. Cognet, I. *et al.* Expression of biologically active mouse ciliary neutrophic factor (CNTF) and soluble CNTFRα in *Escherichia coli* and characterization of their functional specificities. *Eur. Cytokine Netw.* **15,** 255–262 (2004).
31. Howarth, M. *et al.* A monovalent streptavidin with a single femtomolar biotin binding site. *Nature Methods* **3,** 267–273 (2006).
32. Chaiet, L. & Wolf, F. J. The properties of streptavidin, a biotin-binding protein produced by streptomycetes. *Arch. Biochem. Biophys.* **106,** 1–5 (1964).
33. Wall, S. T. *et al.* Multivalency of sonic hedgehog conjugated to linear polymer chains modulates protein potency. *Bioconjug. Chem.* **19,** 806–812 (2008).
34. Tropepe, V. *et al.* Retinal stem cells in the adult mammalian eye. *Science* **287,** 2032–2036 (2000).
35. Ruoslahti, E. & Pierschbacher, M. D. New perspectives in cell adhesion: RGD and integrins. *Science* **238,** 491–497 (1987).
36. Mill, P. *et al.* Sonic hedgehog-dependent activation of Gli2 is essential for embryonic hair follicle development. *Genes Dev.* **17,** 282–294 (2003).
37. Singer, V., Jones, L., Yue, S. & Haugland, R. Characterization of PicoGreen reagent and development of a fluorescence-based solution assay for double-stranded DNA quantitation. *Anal. Biochem.* **249,** 228–238 (1997).
38. Coles, B. L. K., Horsford, D. J., McInnes, R. R. & Kooy, D. Loss of retinal progenitor cells leads to an increase in the retinal stem cell population *in vivo*. *Eur. J. Neurosci.* **23,** 75–82 (2006).
39. Peterson, W. M., Wang, Q., Tzekova, R. & Wiegand, S. J. Ciliary neurotrophic factor and stress stimuli activate the Jak-STAT pathway in retinal neurons and glia. *J. Neurosci.* **20,** 4081–4090 (2000).

Acknowledgements

We are grateful to the Natural Sciences and Engineering Research Council (NSERC) and the Canadian Institutes of Health Research (CIHR) for funding through the Collaborative Health Research Program (CHRP, M.S.S., C.M.M.) and to CIHR for MOP-6279 (K.L.M.). We are also grateful to Le Fonds Québécoise de la recherche sur la nature et les technologies and Vision Science Research Program for financial support (R.G.W.). We thank members of the Shoichet research laboratory for discussions, particularly M. Cooke, S. Owen and K. Ho. We would also like to thank D. Bona for advice with protein expression and purification, R.G.W. Hartley for supplying a barnase expression plasmid (no 8621 pMT1002) through Addgene and J. F. Gauchat for gifting the CNTF plasmid with the biotinylation sequence.

Author contributions

R.G.W.—concept and design, fabrication of all gels, carried out all patterning experiments, collection and assembly of all data, data analysis and interpretation, manuscript writing, final approval of manuscript; S.A.—carried out, collected and analysed all bioactivity experiments; Y.A.—carried out all 3D cell migration studies; K.L.M.—concept and design for barstar–barnase, manuscript writing; C.M.M.—concept and design, data analysis and interpretation, manuscript writing; M.S.S.—concept and design, data analysis and interpretation, manuscript writing, final approval of manuscript.

Additional information

The authors declare no competing financial interests. Supplementary information accompanies this paper on www.nature.com/naturematerials. Reprints and permissions information is available online at http://www.nature.com/reprints. Correspondence and requests for materials should be addressed to M.S.S.